International Journal of Thermophysics, Vol. 13, No. 1, 1992

Radiance Temperatures (in the Wavelength Range 522–906 nm) of Niobium at Its Melting Point by a Pulse-Heating Technique[1]

A. Cezairliyan[2] and A. P. Miiller[2]

Radiance temperatures (at six wavelengths in the range 522–906 nm) of niobium at its melting point were measured by a pulse-heating technique. The method is based on rapid resistive self-heating of the specimen from room temperature to its melting point in less than 1 s and on simultaneously measuring the specimen radiance temperatures every 0.5 ms with a high-speed multiwavelength pyrometer. Melting was manifested by a plateau in the radiance temperature-versus-time function for each wavelength. The melting-point radiance temperatures for a given specimen were determined by averaging the measured temperatures along the plateau at each wavelength (standard deviation of an individual temperature from the mean: 0.1–0.4 K). The melting-point radiance temperatures for niobium were determined, by averaging the results at each wavelength for 10 specimens (standard deviation: 0.3 K), as follows: 2497 K at 522 nm, 2445 K at 617 nm, 2422 K at 653 nm, 2393 K at 708 nm, 2337 K at 809 nm, and 2282 K at 906 nm. Based on estimates of the random and systematic errors arising from pyrometry and specimen conditions, the total error in the reported values is about 5 K at 653 nm and 6 K at the other wavelengths.

KEY WORDS: high-speed pyrometry; high temperature; melting; multiwavelength pyrometry; pulse heating; niobium; radiance temperature.

1. INTRODUCTION

For over two decades, rapid pulse-heating techniques have been used to measure accurately selected thermophysical properties of a number of

[1] Paper presented at the Second Workshop on Subsecond Thermophysics, September 20–21, 1990, Torino, Italy.

[2] Thermophysics Division, National Institute of Standards and Technology, Gaithersburg, Maryland 20899, U.S.A.

0195-928X/92/0100-0039$06.50/0

metals and graphitic materials at high temperatures [1, 2]. Limited measurements on one such property, namely, the radiance temperature[3] of a metal at its melting point, have created considerable interest in that the radiance temperature was found to be essentially constant during the initial melting period and very reproducible for different specimens of the same metal, usually within a few degrees kelvin. It has been suggested [3] that melting-point radiance temperatures of selected metals may provide the basis for high-temperature references which can be easily realized for secondary calibrations of optical pyrometers. However, since most pyrometers operate at wavelengths in the range 400–1000 nm, secondary calibrations would require an accurate knowledge of wavelength dependence of the melting-point radiance temperatures of the selected metals. In an effort to explore the possible development of secondary temperature references, a high-speed multiwavelength pyrometer capable of simultaneously measuring radiance temperature at six wavelengths (nominally in the range 500–900 nm) was constructed at the National Institute of Standards and Technology (NIST) [4].

In the present work, the multiwavelength pyrometer was used to measure the radiance temperatures, at six wavelengths in the range 522–906 nm, of niobium at its melting point. The measurement method was based on passing a large electrical current pulse through the specimen, causing it to undergo rapid resistive self-heating from room temperature to its melting point in less than 1 s, while simultaneously measuring the specimen radiance temperatures every 0.5 ms. The melting-point radiance temperatures for a given specimen were determined by averaging the measured temperatures along the plateau in each radiance temperature versus time function. The melting-point radiance temperatures for niobium were determined by averaging the results for 10 specimens.

2. MEASUREMENT SYSTEM

Figure 1 presents a functional diagram of the high-speed measurement system which includes an electric power-pulsing circuit and its associated measuring and control circuits, a high-speed multiwavelength pyrometer, and a digital data acquisition system.

The power-pulsing circuit consists of the specimen in series with a battery bank, an adjustable resistor (water-cooled Inconel tube), and a fast-acting switch. The battery bank voltage (up to 48 V) and the length

[3] Radiance temperature (sometimes referred to as brightness temperature) of the specimen surface is the temperature at which a blackbody has the same radiance as the surface, corresponding to the effective wavelength of the measuring pyrometer.

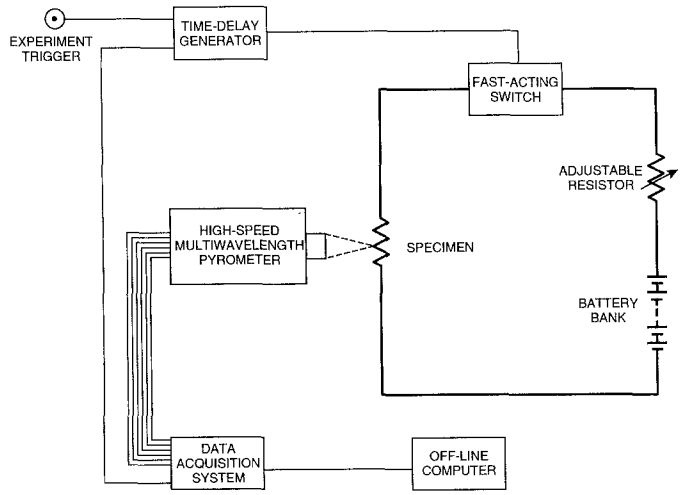

Fig. 1. Functional diagram of the high-speed measurement system.

(hence, resistance) of an Inconel tube in the circuit are adjusted, prior to each pulse experiment, to yield a desired heating rate for the specimen. The timing of various events, such as closing/opening the switch and triggering of the electronic instruments, is achieved by means of time-delay pulse generators. Details concerning the construction and operation of the basic pulse-heating system are given in earlier publications [5, 6].

The high-speed multiwavelength pyrometer [4] is capable of measuring radiance temperatures of a rapidly heating specimen with a time response as fast as 50 μs. The pyrometer lens system focuses the radiance from a circular target area (0.5-mm diameter) on the specimen onto the head of a fiber optic bundle, which is randomly hexfurcated in order to distribute nearly equal fractions of target radiance among six channels. In each channel, the radiance is directed through an interference filter onto a silicon photodiode and the photocurrent from the diode is converted by a high-stability amplifier to a proportionate voltage.

Figure 2 presents the relative spectral transmittance of the pyrometer, which, for each channel, includes the combined transmittance of all optical components (lens system, fiber optics, and interference filter) in front of the photodiode. The principal channel upon which the pyrometer calibration (Section 3) is based has a bandwidth of 26 nm centered at 653 nm; the bandwidths of the other five channels, centered nominally at 500, 600, 700, 800, and 900 nm, are in the range 54–78 nm.

The digital data acquisition system utilizes (i) six track/hold amplifiers to read simultaneously the voltage signals from the pyrometer channels at

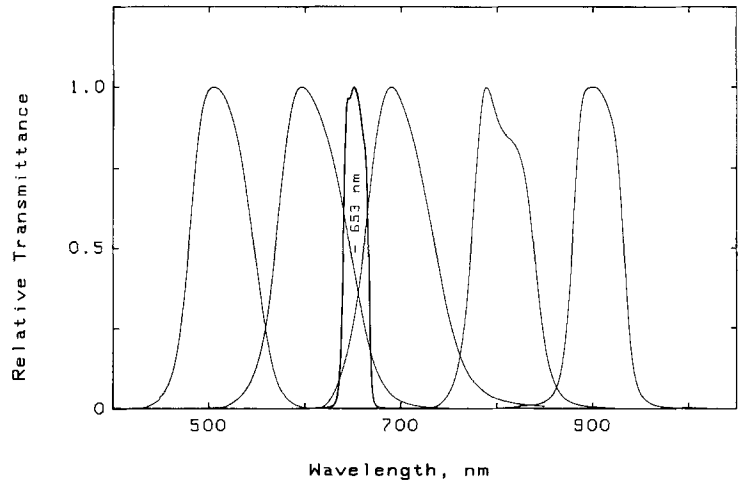

Fig. 2. Relative transmittance of the six channels in the multiwavelength pyrometer.

selectable rates of up to 15 kHz and (ii) a high-speed voltmeter to scan rapidly the amplifiers, digitize the analog signals with 13-bit resolution, and store the digital data in its memory (64 kbytes).

3. MEASUREMENTS

The radiance temperature measurements were performed on 10 specimens of 99.9 + % pure niobium in the form of strips with the following nominal dimensions: length, 50 mm; width, 6.3 mm; and thickness, 0.13 mm. A typical analysis by the manufacturer of the stock material indicated the presence of the following impurities (in ppm by mass): Zr, 100; Fe, Hf, O, and Si, 50 each; C, Cu, and Ti, 40 each; N, 26; Al, Cr, Ca, Mg, Mn, Mo, Ni, Pb, and V, 20 each; Co, Sn, and W, 10 each; H, Cd, 5 each; and B, 1.

The multiwavelength pyrometer was calibrated, prior to the pulse-heating experiments, in two steps [4]. First the 653-nm channel was calibrated with a tungsten-filament standard lamp, which, in turn, had been calibrated against the NIST Photoelectric Pyrometer by the Radiometric Physics Division at NIST. Then the temperature calibration of the 653-nm channel was transferred to the other five channels by performing (steady-state) measurements on a graphite tube blackbody furnace. All temperatures reported in this paper, except where explicitly noted otherwise, are based on the International Temperature Scale of 1990 (ITS-90) [7].

For pulse heating, each specimen strip was mounted vertically between two electrodes inside the experiment chamber; the upper electrode is stationary, whereas the lower electrode is attached to a flexible connection to allow for thermal expansion of the specimen during heating. The chamber was evacuated and then filled with argon gas at a pressure of approximately 0.1 MPa in order to minimize evaporation of the niobium specimen at high temperatures.

Prior to each experiment, adjustments were made to the battery bank voltage and to the resistor in series with the specimen in order to achieve a desired heating rate. The specimen was then rapidly heated from room temperature to its melting point in less than 1 s by passing a large electrical current pulse through it; the heating periods (from room temperature to the melting point) ranged from about 210 to 690 ms. During the experiment, the six pyrometer signals were digitized and recorded simultaneously every 0.5 ms by the data acquisition system. After the experiment, the recorded data were transferred to a minicomputer for subsequent analyses to determine the radiance temperatures.

Figure 3 illustrates the variation of radiance temperature corresponding to six effective wavelengths[4] as a function of time near and at the melting point of niobium during a typical pulse-heating experiment.

[4] The effective wavelength for each pyrometer channel was determined following the method of Kostkowski and Lee [8], which takes into account the spectral distribution of the specimen radiance as well as the spectral transmittance of each channel.

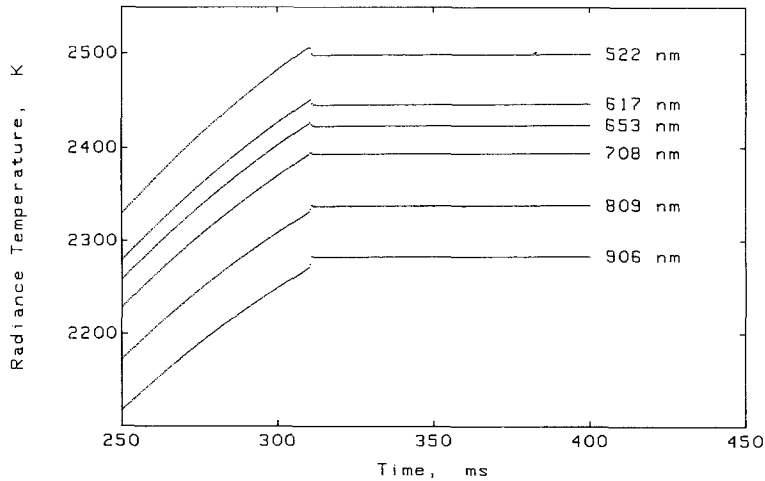

Fig. 3. Variation of the radiance temperatures of a niobium strip specimen just before and during melting as measured by the multiwavelength pyrometer. The effective wavelength, shown for each channel, was determined by the method of Kostkowski and Lee [8].

Table I. A Summary of Measurements of Radiance Temperature (in the Wavelength Range 522 to 906 nm) of Niobium at Its Melting Point

Specimen[a]	Effective wavelength[b] (nm)	Premelting heating rate[c] ($K \cdot s^{-1}$)	Melting period				
			Number of temperatures[d]	Slope at plateau[e] ($K \cdot s^{-1}$)	Plateau temp. difference[f] (K)	Plateau radiance temp.[g] (K)	SD[h] (K)
1	522	2590	221	11.6	1.3	2497.7	0.4
	617	2520	221	12.6	1.4	2444.9	0.4
	653	2490	221	11.4	1.2	2422.8	0.4
	708	2450	221	11.0	1.2	2392.5	0.4
	809	2370	221	9.7	1.1	2336.4	0.3
	906	2300	221	7.0	0.8	2281.8	0.2
2	522	650	611	3.5	1.1	2497.9	0.3
	617	640	611	3.9	1.2	2445.2	0.3
	653	630	611	3.3	1.0	2423.0	0.3
	708	620	611	2.7	0.8	2393.0	0.3
	809	600	611	0.9	0.3	2337.1	0.2
	906	580	611	−1.1	−0.3	2282.1	0.2
3	522	1090	181	4.6	0.4	2497.3	0.1
	617	1060	181	5.2	0.5	2444.6	0.1
	653	1040	181	4.6	0.4	2422.3	0.1
	708	1020	181	5.0	0.4	2392.4	0.1
	809	980	181	3.8	0.3	2336.5	0.1
	906	950	181	2.4	0.2	2281.7	0.1
4	522	3970	121	15.6	0.9	2497.2	0.3
	617	3860	121	15.5	0.9	2444.6	0.3
	653	3780	121	13.4	0.8	2422.3	0.3
	708	3720	121	13.4	0.8	2392.5	0.2
	809	3570	121	12.9	0.8	2336.7	0.2
	906	3460	121	11.8	0.7	2281.9	0.2
5	522	4340	93	22.4	1.0	2497.3	0.3
	617	4230	93	19.5	0.9	2444.6	0.3
	653	4150	93	18.7	0.9	2422.3	0.3
	708	4090	93	15.8	0.7	2392.4	0.2
	809	3920	93	9.9	0.5	2336.7	0.2
	906	3800	93	3.6	0.2	2281.8	0.1

6	522	2890	111	3.1	0.2	2497.4	0.1
	617	2800	111	1.1	0.1	2444.7	0.1
	653	2740	111	−0.3	0.0	2422.5	0.1
	708	2690	111	−2.4	−0.1	2392.6	0.1
	809	2590	111	−0.4	0.0	2336.9	0.1
	906	2480	111	2.2	0.1	2282.0	0.1
7	522	370	531	3.3	0.9	2497.2	0.3
	617	360	531	2.9	0.8	2444.5	0.2
	653	360	531	2.5	0.7	2422.2	0.2
	708	350	531	1.8	0.5	2392.3	0.1
	809	340	531	1.1	0.3	2336.5	0.1
	906	330	531	0.1	0.0	2281.6	0.1
8	522	2510	171	15.6	1.3	2497.8	0.4
	617	2440	171	17.1	1.5	2445.2	0.4
	653	2390	171	15.9	1.3	2422.9	0.4
	708	2360	171	14.8	1.3	2393.1	0.4
	809	2250	171	14.2	1.2	2337.3	0.4
	906	2180	171	13.6	1.2	2282.3	0.3
9	522	820	241	4.2	0.5	2497.4	0.2
	617	800	241	2.6	0.3	2444.9	0.1
	653	790	241	1.5	0.2	2422.5	0.1
	708	780	241	1.3	0.2	2392.7	0.1
	809	760	241	1.0	0.1	2337.0	0.1
	906	730	241	1.4	0.2	2282.0	0.1
10	522	2790	131	4.1	0.3	2497.4	0.1
	617	2710	131	3.6	0.2	2444.6	0.1
	653	2660	131	1.4	0.1	2422.2	0.1
	708	2620	131	2.6	0.2	2392.4	0.1
	809	2520	131	−2.5	−0.2	2336.6	0.1
	906	2450	131	−2.9	−0.2	2281.7	0.1

[a] Also represents the experiments in chronological order.
[b] Determined by the method of Kostkowski and Lee [8].
[c] Heating rate evaluated at a temperature approximately 15 K below the plateau radiance temperature.
[d] Number of temperatures at the plateau averaged to obtain the plateau radiance temperature.
[e] Derivative of the temperature versus time function obtained by (least-squares) fitting a linear function in time to the temperature data at the plateau.
[f] Radiance temperature difference between the beginning and the end of the plateau based on the linear temperature-versus-time function.
[g] Average value (for a given specimen and given effective wavelength) of the measured radiance temperatures at the plateau.
[h] Standard deviation of an individual temperature from the plateau radiance temperature.

The melting of the specimen is manifested by a plateau in the radiance versus time function at each wavelength. A more detailed view of the plateau region, presented in Fig. 4, indicates the presence of a small slope corresponding to a temperature difference between the beginning and the end of the plateau of about 1 K. At the beginning of the melting plateaus there are abrupt changes in radiance temperature (about 10 K or less) which suggest a sudden decrease (at the short wavelengths) or increase (at long wavelengths) in the normal spectral emissivity of the niobium surface at the onset of melting.

4. RESULTS

The results obtained from pulse-heating experiments on 10 niobium specimens are summarized in Table I. For a given specimen, the plateau radiance temperature, at each effective wavelength, was determined by averaging the measured temperatures along the flat portion of the corresponding plateau (indicated by the dashed lines in Fig. 4). The number of temperatures used for averaging ranged from 93 to 701, depending on the heating rate and the behavior of the specimen during melting. The standard deviation of an individual temperature from the average is in the range 0.1–0.4 K for all 10 experiments.

The trend of radiance temperature along each plateau was determined by fitting the measured temperatures by a linear function of time with the least-squares method. The temperature difference between the beginning and the end of the plateau, as determined from the slope of the linear functions, is in the range -0.6 to 1.5 K.

The specimen heating rates were determined by fitting linear functions of time to the radiance temperatures measured during the premelting period. The heating rates (slopes of the linear functions approximately 15 K below the melting plateaus) range from 320 to 4340 $K \cdot s^{-1}$ (Table I). The plateau radiance temperatures (corresponding to 10 specimens/experiments) at each effective wavelength are plotted against heating rate in Fig. 5. As may be seen, the plateau radiance temperature does not depend on heating rate.

Table II presents the final results for the radiance temperature of niobium at its melting point that were obtained by averaging, at each effective wavelength, the values of plateau radiance temperature for 10 specimens given in Table I. The standard deviation of an individual plateau radiance temperature from the average is 0.3 K and the maximum absolute deviation is 0.6 K. Also given in Table II are the corresponding values for the normal spectral emissivity of niobium at its melting point that were

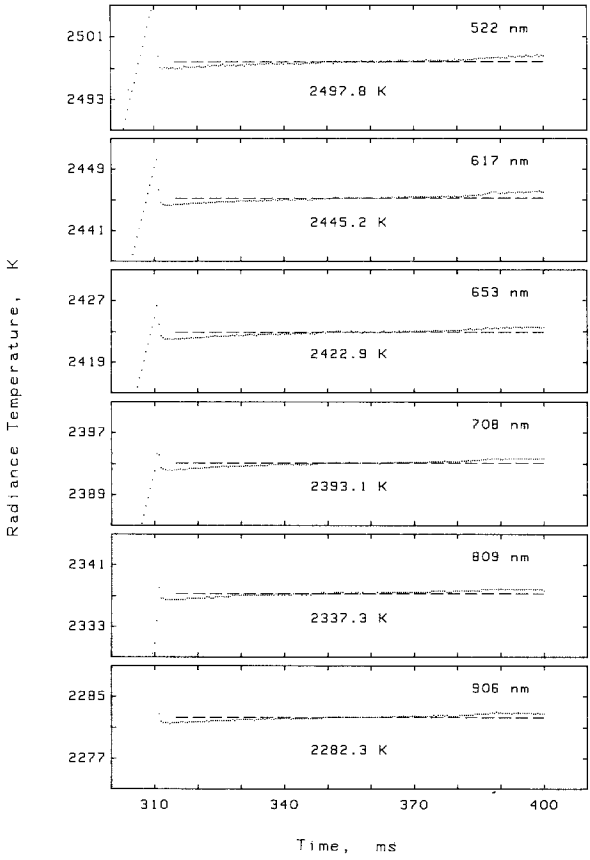

Fig. 4. Expanded plot of the radiance temperature-versus-time functions shown in Fig. 3. Each dashed line (and labeled temperature) indicates the average temperature along the plateau (or melting-point radiance temperature) at a given wavelength.

calculated by means of Planck's law, based on the present results for radiance temperature and the value of 2749 K (on ITS-90) for the melting point of niobium [9].

5. ESTIMATE OF ERRORS

A detailed analysis of sources and magnitudes of the random and systematic errors in temperature measurements with the multiwavelength pyrometer is given elsewhere [4]. The major error sources arise from (i) the calibration and operation of the pyrometer and (ii) the physical/chemi-

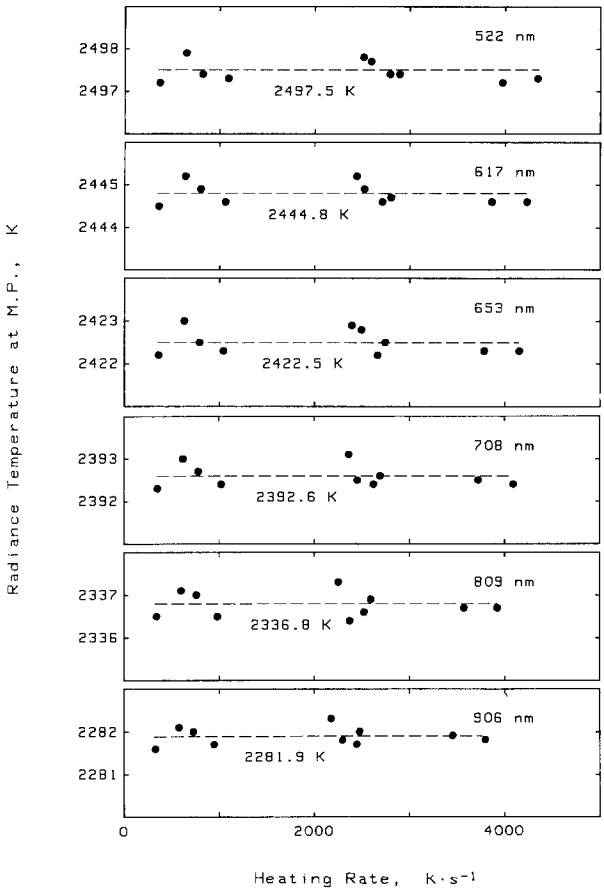

Fig. 5. Melting-point radiance temperatures as a function of the heating rate used in 10 experiments. Each dashed line (and labeled temperature) indicates the average melting-point radiance temperature (at a given wavelength) for the 10 niobium specimens.

cal conditions and melting behavior of each specimen. A summary of the estimated uncertainties in the reported radiance temperatures is presented in Table III.

6. DISCUSSION

There have been only a limited number of investigations that have yielded data on the radiance temperature of niobium at its melting point. These investigations reported measurements of either (i) radiance tem-

Table II. Final Results for the Average Radiance Temperature[a] and Normal Spectral Emissivity (at Six Wavelengths) of Niobium at Its Melting Point

Effective wavelength[b] (nm)	Radiance temperature[c] (K)	SD[d] (K)	Max. abs. deviation (K)	Normal spectral emissivity[e]
522	2497.5	0.3	0.5	0.364
617	2444.8	0.3	0.5	0.348
653	2422.5	0.3	0.6	0.339
708	2392.6	0.3	0.5	0.332
809	2336.8	0.3	0.6	0.319
906	2281.9	0.2	0.4	0.306

[a] Temperature based on the International Temperature Scale of 1990.
[b] Determined by the method of Kostkowski and Lee [8].
[c] Average of the plateau radiance temperatures at each effective wavelength for 10 niobium specimens (Table I).
[d] Standard deviation of an individual plateau radiance temperature from the average plateau radiance temperature.
[e] Determined by means of Planck's law from the average plateau radiance temperature and the value 2749 K (on ITS-90) for the melting point of niobium [9].

Table III. Sources and Magnitudes of Inaccuracies in the Measurement of Radiance Temperature Near 2500 K with the Multiwavelength Pyrometer (Operating in the Range 522 to 906 nm) at NIST

	Inaccuracy (K) at effective wavelength (nm)					
Source	522	617	653	708	809	906
Pyrometry						
Standard lamp calibration	2	2	2	2	2	2
Drift in standard lamp calibration	1	1	1	1	1	1
Radiation source alignment	2	2	2	2	2	2
Window calibration	1	1	1	1	1	1
Effective wavelength	3	3	1	3	3	3
Pyrometer signal noise	1	1	1	1	1	1
Pyrometer calibration drift	2	2	2	2	2	2
Calibration transfer (blackbody furnace)	2	2	0	2	2	2
Specimen-related						
Impurities	1	1	1	1	1	1
Melting behavior	2	2	2	2	2	2
Total Inaccuracy (root sum square of above items)	6	6	5	6	6	6

perature or (ii) normal spectral emissivity, which, in conjunction with an independent knowledge of melting temperature, enabled the calculation of a corresponding radiance temperature via Planck's law. These melting-point radiance temperatures are listed along with the present results in Table IV. A comparison (based on ITS-90) of the literature data with the present work is given in Fig. 6. The present results are shown as filled circles joined by straight-line segments.

Several investigators have used conventional optical pyrometry to measure melting-point radiance temperatures of niobium in experiments which utilized electromagnetic levitation/induction heating techniques. The earliest measurements appear to be those of Bonnell et al. [10], who

Table IV. Radiance Temperatures at Wavelengths (λ) in the Range 500–1000 nm of Niobium at Its Melting Point as Reported in the Literature

Investigator(s)	Ref. No.	Year	Purity (wt. %)	Heating method[a]	λ (nm)	Radiance temperature (K)	
						As reported	On ITS-90
Bonnell et al.	10	1972	99.9	E	645	2405 ± 7	2404 ± 7
Cezairliyan	16	1973	99.9+	R	650	2425 ± 10	2424 ± 10
Berezin et al.	11	1976	99.76	E	650	2434 ± 6	2433 ± 6
Righini	17	1980	99.99	R	658	2421	2420
Betz and Frohberg	12	1980	99.96	E	547	2487	2486
					650	2432	2431
Hiernaut et al.	14	1989	99.84	L	500		2467[b]
					650		2393[b]
					1000		2238[b]
Righini	18	1990	99.9+	R	897	2286	2286
Krishnan et al.	13		99.99	E	632.8		2417[c]
Present work			99.9+	R	522		2497 ± 6
					617		2445 ± 6
					653		2422 ± 5
					708		2393 ± 6
					809		2337 ± 6
					906		2282 ± 6

[a] Method used to heat the specimen (specimen geometry in parentheses): R, resistive self-heating (flat strip); E, electromagnetic levitation/induction heating (sphere); L, laser pulse heating (sphere).

[b] Based on the constant emissivity (0.30 for the wavelength range 500–1000 nm) and the melting temperature (2751 K on ITS-90) reported by the investigators.

[c] Based on the emissivity (0.321) reported by the investigators and a melting temperature of 2749 K (on ITS-90) for niobium [9].

obtained a value (see Table IV) that is about 23 K lower than the interpolated value (at 645 nm) based on the present results; this difference is somewhat greater than the combined uncertainties in the two investigations. Subsequent levitation experiments by Berezin et al. [11] and by Betz and Frohberg [12] have yielded values that are about 10 K or less higher than the present values, differences that are within the combined experimental uncertainties of radiance temperature measurements.

Recently, Krishnan et al. [13] have used laser ellipsometry in conjunction with electromagnetic levitation/induction heating to measure normal spectral emissivities (at 632.8 nm) of niobium in both its solid and its liquid phases. The emissivity of niobium at the melting point was determined to be 0.321. This emissivity value and a melting temperature of 2749 K (on ITS-90) for niobium [9] yield a melting-point radiance temperature (see Table IV) that is about 17 K below the interpolated value (at 633 nm) based on the present results. This difference, though somewhat large, is of the order of the combined maximum possible experimental uncertainties associated with their emissivity measurements ($\pm 1\%$), our radiance temperature measurements (± 6 K), and the value for melting temperature (± 10 K).

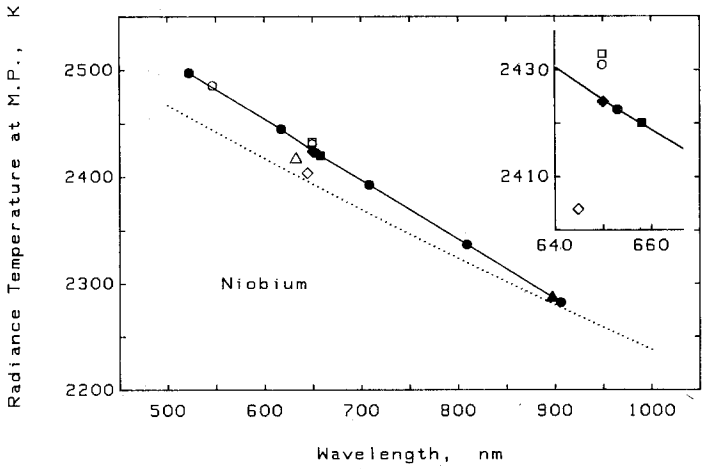

Fig. 6. Comparison (on ITS-90) of literature values and present results for the radiance temperature of niobium at its melting point. The different symbol types refer to different methods used for specimen heating, as follows: filled symbols, rapid resistive self-heating; open symbols, electromagnetic levitation/induction heating; dotted curve, laser pulse heating. The specific symbols designating the data correspond to the references as follows: ◇, Bonnell et al. [10]; □, Berezin et al. [11]; ○, Betz and Frohberg [12]; △, Krishnan et al. [13]; · · · · ·, Hiernaut et al. [14]; ◆, Cezairliyan [16]; ■, Righini [17]; ▲, Righini [18]; ●, present work.

In a study of several high-temperature metals (including V, Nb, Mo, Ta, and W) by laser pulse heating, Hiernaut et al. [14] used a different approach to obtain values for normal spectral emissivity ($\varepsilon_{N,\lambda}$) from measurements of specimen radiance with a six-wavelength pyrometer. They assumed $\ln \varepsilon_{N,\lambda}$ to be a linear function of wavelength and introduced this expression into Planck's radiation equation, resulting in six equations for the six wavelengths. The pairwise combination of these equations leads to an overdetermined system of 15 equations from which true temperature and $\varepsilon_{N,\lambda}$ were determined by least-squares fitting techniques. Their "fitted" results indicate that $\varepsilon_{N,\lambda}$ at the melting point of not only niobium but all the high-temperature metals studied is constant, independent of wavelength, over the wavelength range 500–1000 nm.

The constant emissivity value (0.30) obtained by Hiernaut et al. for niobium is in significant disagreement with the present results (Table II), which show that the melting-point emissivity of niobium changes by more than 15% between wavelengths 522 and 906 nm, a difference which is significantly larger than could be realistically attributed to temperature measurement error. For example, an uncertainty of 6 K in radiance temperature corresponds to an uncertainty of less than 3% in emissivity. Furthermore, a recent review [15] of literature data has concluded that the normal spectral emissivities of several high-temperature metals (Ni, Ti, V, Nb, Mo, Ta, and W) at their melting point are clearly not constant but all decrease monotonically with increasing wavelength in the range 400–1000 nm.

As may be seen in Fig. 6, the radiance temperatures (dotted curve) that were calculated (via Planck's law) from the "fitted" results reported by Hiernaut et al. for melting temperature and emissivity are systematically lower (by about 5 K at 900 nm increasing to about 50 K at 500 nm) than the present results, which were determined directly from measurements of specimen radiance via Planck's radiation equation. Unfortunately, Hiernaut et al. did not report any radiance temperatures which, in principle, could have been determined directly from their measurements of specimen radiance.

Other investigations have also used high-speed pyrometry in conjunction with rapid pulse-heating techniques to measure the melting-point radiance temperatures of niobium strip specimens. As may be seen in Fig. 6 (inset), earlier measurements at single wavelengths near 650 nm at NIST by Cezairliyan [16] and at the Istituto di Metrologia "G. Colonnetti" (IMGC) by Righini [17] are in excellent agreement with the present work (within 1 K). Recent measurements at 897 nm by Righini [18] at the IMGC are also in very good agreement, within approximately 1 K of the interpolated value (at 897 nm) based on the present results (see Table IV).

The excellent agreement among values measured near 650 and 900 nm at NIST and IMGC is particularly noteworthy since the measurements span nearly 20 years and involve three high-speed pyrometers of very different design, two pulse-heating systems, and two temperature calibration schemes. At NIST, the high-speed single-wavelength pyrometer [19] and the present high-speed multiwavelength pyrometer [4] are calibrated near 650 nm by means of a tungsten filament reference lamp which, in turn, is calibrated against the NIST photoelectric pyrometer. A graphite blackbody furnace is used to transfer the calibration of the multiwavelength pyrometer near 650 nm to the other wavelengths. At IMGC, the high-speed pyrometer [20], which operates as a monochromatic instrument with interchangeable interference filters, is calibrated on the basis of measurements of its effective wavelength, the signal at a reference temperature (gold freezing point), and the linearity of the detector.

Possible effects of specimen bulk impurities and/or specimen surface contaminants (oxides, nitrides) on the radiance temperature measurements at NIST and at IMGC are believed to be minimal for several reasons: (i) the niobium specimens were fabricated from different lots of material (99.9 + % pure), supplied by two manufacturers; (ii) measurements that were performed on specimens with untreated surfaces and with surfaces that had been mechanically abraded to different roughnesses yielded very reproducible results, to within ± 2 K [16, 17]; and (iii) measurements performed in the present work at heating rates differing by as much as one order of magnitude (approximately 400–4000 $K \cdot s^{-1}$), thereby exposing the specimens to elevated temperatures for short yet different durations (from several tens to a few hundred milliseconds), also yield highly reproducible results, to within ± 1 K. The good agreement among results for specimens with untreated surfaces and those with mechanically abraded surfaces suggests that there were no significant preexisting surface contaminants on the niobium strip specimens. The excellent agreement among results obtained at different heating rates suggests that there was minimal contamination of the specimen surface by residual impurities in the argon gas environment during the short duration experiments.

7. CONCLUDING REMARKS

The present work on niobium has shown that measurements, repeated on several strip specimens, yield highly reproducible results (within about 1 K), for the melting-point radiance temperatures at six wavelengths. Furthermore, similar pulse-heating experiments involving different measurement and calibration systems at different laboratories also tend to yield reproducible results.

Because of the simplicity and ease of performing pulse experiments on metal strips, radiance temperatures at the melting point of selected metals are likely to form the necessary foundation for temperature references which can be easily realized for high-temperature optical pyrometry. This would be particularly attractive for rapid secondary calibrations of pyrometers in environments where lengthy primary calibration procedures are either undesirable or not possible (microgravity research, industrial high-temperature technologies, etc.). However, applications to conventional pyrometry (time response 1 s or slower) would require the development of techniques for maintaining a stable specimen surface for several seconds during melting.

In the future, accurate measurements of radiance temperature (over a range 500–1000 nm) at the melting point of several other high-temperature metals will be required to cover a sufficient temperature range for the establishment of secondary temperature reference points.

ACKNOWLEDGMENTS

This work was supported in part by the Microgravity Science and Applications Division of NASA. The authors are grateful to R. F. Chang for performing the measurements of spectral transmittance of the multi-wavelength pyrometer. The authors also gratefully acknowledge the helpful comments and suggestions by D. Bonnell.

REFERENCES

1. A. Cezairliyan, *Int. J. Thermophys.* **5**:177 (1984).
2. F. Righini, G. C. Bussolino, and A. Rosso, in *Proceedings of the Australasian Instrumentation Conference AIM-89* (The Institution of Engineers, Australia, Barton, ACT, 1989), pp. 144–150.
3. A. Cezairliyan, A. P. Miiller, F. Righini, and A. Rosso, in *Temperature: Its Measurement and Control in Science and Industry, Vol. 5*, J. F. Schooley, ed. (AIP, New York, 1982), Part 1, pp. 377–381.
4. A. Cezairliyan, G. M. Foley, M. S. Morse, and A. P. Miiller, in *Temperature: Its Measurement and Control in Science and Industry, Vol. 6* (in preparation).
5. A. Cezairliyan, M. S. Morse, H. A. Berman, and C. W. Beckett, *J. Res. Natl. Bur. Stand. (U.S.)* **74A**:65 (1970).
6. A. Cezairliyan, *J. Res. Natl. Bur. Stand. (U.S.)* **75C**:7 (1971).
7. H. Preston-Thomas, *Metrologia* **27**:3, 107 (1990).
8. H. J. Kostkowski and R. D. Lee, in *Temperature: Its Measurement and Control in Science and Industry, Vol. 3*, C. M. Hertzfeld, ed. (Reinhold, New York, 1962), Part 1, pp. 449–481.
9. A. Cezairliyan, *High Temp. High Press.* **4**:453 (1972).

10. D. W. Bonnell, J. A. Treverton, A. J. Valerga, and J. L. Margrave, in *Temperature: Its Measurement and Control in Science and Industry, Vol. 4*, H. H. Plumb, ed. (ISA, Pittsburgh, 1972), Part 1, pp. 483–487.
11. B. Ya. Berezin, S. A. Kats, and V. Ya. Chekhovskoi, *High Temp. (USSR)* **14**:448 (1976).
12. G. Betz and M. G. Frohberg, *Z. Metallkde.* **71**:451 (1980).
13. S. Krishnan, J. K. R. Weber, P. C. Nordine, R. A. Schiffman, R. H. Hauge, and J. L. Margrave, *High Temp. Sci.* (in press).
14. J. P. Hiernaut, F. Sakuma, and C. Ronchi, *High Temp. High Press.* **21**:139 (1989).
15. A. Cezairliyan, A. P. Miiller, F. Righini, and A. Rosso, *High Temp. High Press.* (in press).
16. A. Cezairliyan, *J. Res. Natl. Bur. Stand. (U.S.)* **77A**:333 (1973).
17. F. Righini, Unpublished data (1980).
18. F. Righini, Unpublished data (1990).
19. G. M. Foley, *Rev. Sci. Instrum.* **41**:827 (1970).
20. L. Coslovi, F. Righini, and A. Rosso, *Alta Frequenza* **44**:592 (1975).